Real time dynamic strain monitoring of optical links using the backreflection of live PSK data

H. F. MARTINS,[1,*] K. SHI,[2] B. C. THOMSEN,[2] S. MARTIN-LOPEZ,[3] M. GONZALEZ-HERRAEZ,[3] AND S. J. SAVORY[4]

[1]*FOCUS S. L., C/ Orellana, 1, 1° Izquierda, 28804, Madrid, Spain*
[2]*Optical Networks Group, Department of Electrical and Electronic Engineering, University College London, Torrington Place, London, WC1E 7JE, UK*
[3]*Departamento de Electrónica, Universidad de Alcalá, Escuela Politécnica Superior, 28805, Madrid, Spain*
[4]*Department of Engineering, University of Cambridge, Cambridge, CB2 1PZ, UK*
[*]*hugo.martins@focustech.eu*

Abstract: A major cause of faults in optical communication links is related to unintentional third party intrusions (normally related to civil/agricultural works) causing fiber breaks or cable damage. These intrusions could be anticipated and avoided by monitoring the dynamic strain recorded along the cable. In this work, a novel technique is proposed to implement real-time distributed strain sensing in parallel with an operating optical communication channel. The technique relies on monitoring the Rayleigh backscattered light from optical communication data transmitted using standard modulation formats. The system is treated as a phase-sensitive OTDR (ΦOTDR) using random and non-periodical non-return-to-zero (NRZ) phase-shift keying (PSK) pulse coding. An I/Q detection unit allows for a full (amplitude, phase and polarization) characterization of the backscattered optical signal, thus achieving a fully linear system in terms of ΦOTDR trace coding/decoding. The technique can be used with different modulation formats, and operation using 4 Gbaud single-polarization dual PSK and 4 Gbaud dual-polarization quadrature PSK is demonstrated. As a proof of concept, distributed sensing of dynamic strain with a sampling of 125 kHz and a spatial resolution of 2.5 cm (set by the bit size) over 500 m is demonstrated for applied sinusoidal strain signals of 500 Hz. The limitations and possibilities for improvement of the technique are also discussed.

References and links

1. X. Bao and L. Chen, "Recent progress in distributed fiber optic sensors," Sensors (Basel) **12**(7), 8601–8639 (2012).
2. G. Bolognini, J. Park, M. A. Soto, N. Park, and F. Di Pasquale, "Analysis of distributed temperature sensing based on Raman scattering using OTDR coding and discrete Raman amplification," Meas. Sci. Technol. **18**(10), 3211–3218 (2007).
3. M. A. Soto, T. Nannipieri, A. Signorini, A. Lazzeri, F. Baronti, R. Roncella, G. Bolognini, and F. Di Pasquale, "Raman-based distributed temperature sensor with 1 m spatial resolution over 26 km SMF using low-repetition-rate cyclic pulse coding," Opt. Lett. **36**(13), 2557–2559 (2011).
4. S. Le Floch, F. Sauser, M. A. Soto, and L. Thévenaz, "Time/frequency coding for Brillouin distributed sensors," Proc. SPIE **8421**, 84211J (2012).
5. M. A. Soto, G. Bolognini, and F. Di Pasquale, "Analysis of pulse modulation format in coded BOTDA sensors," Opt. Express **18**(14), 14878–14892 (2010).
6. M. A. Soto, G. Bolognini, F. Di Pasquale, and L. Thévenaz, "Simplex-coded BOTDA fiber sensor with 1 m spatial resolution over a 50 km range," Opt. Lett. **35**(2), 259–261 (2010).
7. X. Angulo-Vinuesa, S. Martin-Lopez, J. Nuño, P. Corredera, J. Diego Ania-Castañon, L. Thévenaz, and M. Gonzalez-Herraez, "Raman-assisted brillouin distributed temperature sensor over 100 km Featuring 2 m resolution and 1.2 °C uncertainty," J. Lightwave Technol. **30**(8), 1060–1065 (2012).
8. M. D. Jones, "Using Simplex codes to improve OTDR Sensitivity," IEEE Photonics Technol. Lett. **15**(7), 822–824 (1993).
9. D. Lee, H. Yoon, P. Kim, J. Park, and N. Park, "Optimization of SNR improvement in the noncoherent OTDR based on simplex codes," J. Lightwave Technol. **24**(1), 322–328 (2006).

10. J. Pastor Graells, H. F. Martins, S. Martin-Lopez, and M. Gonzalez Herraez, "Distributed measurement of vibrations in a ramified fiber structure using phase sensitive optical time domain reflectometry and wavelength routing concepts," in *Advanced Photonics* (2014), paper SeW1C.5.
11. H. F. Martins, S. Martin-Lopez, P. Corredera, M. L. Filograno, O. Frazão, and M. González-Herráez, "Coherent Noise Reduction in High Visibility Phase-Sensitive Optical Time Domain Reflectometer for Distributed Sensing of Ultrasonic Waves," J. Lightwave Technol. **31**(23), 3631–3637 (2013).
12. Z. Qin, L. Chen, and X. Bao, "Wavelet denoising method for improving detection performance of distributed vibration sensor," IEEE Photonics Technol. Lett. **24**(7), 542–544 (2012).
13. L. B. Liokumovich, N. A. Ushakov, O. I. Kotov, M. A. Bisyarin, and A. H. Hartog, "Fundamentals of Optical Fiber Sensing Schemes Based on Coherent Optical Time Domain Reflectometry: Signal Model Under Static Fiber Conditions," J. Lightwave Technol. **33**(17), 3660–3671 (2015).
14. Y. Koyamada, M. Imahama, K. Kubota, and K. Hogari, "Fiber-optic distributed strain and temperature sensing with very high measurand resolution over long range using coherent OTDR," J. Lightwave Technol. **27**(9), 1142–1146 (2009).
15. M. A. Soto, X. Lu, H. F. Martins, M. Gonzalez-Herraez, and L. Thévenaz, "Distributed phase birefringence measurements based on polarization correlation in phase-sensitive optical time-domain reflectometers," Opt. Express **23**(19), 24923–24936 (2015).
16. H. F. Martins, S. Martin-Lopez, P. Corredera, M. L. Filograno, O. Frazão, and M. Gonzalez-Herraez, "Phase-sensitive optical time domain reflectometer assisted by first-order Raman amplification for distributed vibration sensing over >100km," J. Lightwave Technol. **32**(8), 1510–1518 (2014).
17. H. F. Martins, S. Martin-Lopez, P. Corredera, J. D. Ania-Castanon, O. Frazao, and M. Gonzalez-Herraez, "Distributed Vibration Sensing Over 125 km With Enhanced SNR Using Phi-OTDR Over a URFL Cavity," J. Lightwave Technol. **33**(12), 2628–2632 (2015).
18. Z. N. Wang, J. Li, M. Q. Fan, L. Zhang, F. Peng, H. Wu, J. J. Zeng, Y. Zhou, and Y. J. Rao, "Phase-sensitive optical time-domain reflectometry with Brillouin amplification," Opt. Lett. **39**(15), 4313–4316 (2014).
19. Z. N. Wang, J. J. Zeng, J. Li, M. Q. Fan, H. Wu, F. Peng, L. Zhang, Y. Zhou, and Y. J. Rao, "Ultra-long phase-sensitive OTDR with hybrid distributed amplification," Opt. Lett. **39**(20), 5866–5869 (2014).
20. F. Peng, H. Wu, X. H. Jia, Y. J. Rao, Z. N. Wang, and Z. P. Peng, "Ultra-long high-sensitivity Φ-OTDR for high spatial resolution intrusion detection of pipelines," Opt. Express **22**(11), 13804–13810 (2014).
21. A. Masoudi, M. Belal, and T. P. Newson, "A distributed optical fiber dynamic strain sensor based on phase-OTDR," Meas. Sci. Technol. **24**(8), 085204 (2013).
22. Z. Wang, L. Zhang, S. Wang, N. Xue, F. Peng, M. Fan, W. Sun, X. Qian, J. Rao, and Y. Rao, "Coherent Φ-OTDR based on I/Q demodulation and homodyne detection," Opt. Express **24**(2), 853–858 (2016).
23. G. Tu, X. Zhang, Y. Zhang, F. Zhu, L. Xia, and B. Nakarmi, "The Development of an Phi-OTDR System for Quantitative Vibration Measurement," IEEE Photonics Technol. Lett. **27**(12), 1349–1352 (2015).
24. Y. Muanenda, C. J. Oton, S. Faralli, and F. Di Pasquale, "A Cost-Effective Distributed Acoustic Sensor Using a Commercial Off-the-Shelf DFB Laser and Direct Detection Phase-OTDR," IEEE Photonics J. **8**(1), 1–10 (2016).
25. Y. Takushima and Y. C. Chung, "Optical reflectometry based on correlation detection and its application to the in-service monitoring of WDM passive optical network," Opt. Express **15**(9), 5318–5326 (2007).
26. K. Shi and B. C. Thomsen, "Sparse Adaptive Frequency Domain Equalizers for Mode-Group Division Multiplexing," J. Lightwave Technol. **33**(2), 311–317 (2015).

1. Introduction: Distributed fiber optic sensors and optical communications

Distributed optical fiber sensors (DOFS) allow for the distributed monitoring of different physical parameters (temperature, strain, pressure, birefringence) along optical fibers. Due to the need of a single interrogation unit for addressing tens of thousands of measurement points along the fiber, these sensors provide cost-effective solutions for the characterization of links in optical networks and/or real-time monitoring of large civil infrastructures [1].

DOFS can be based on Rayleigh, Brillouin or Raman scattering. Traditionally, Raman and Brillouin-based sensors are associated with static monitoring (measurement times of a few seconds to a few minutes, due to the requirement of a large number of averages) of temperature [2,3] and temperature/strain [4–7], respectively. As for Rayleigh based sensing, noncoherent (i.e., using a low coherence light source) optical time domain reflectometry (OTDR) can be used to characterize the losses or locate fiber breaks [8,9], while phase-sensitive OTDR (ΦOTDR) (i.e., using a highly coherent light source) is typically associated with dynamic sensing of vibrations/intrusions along an optical fiber [10–24].

A number of variations from traditional configurations based on Raman/Brillouin/Rayleigh scattering and aimed at different types of operation can be found in the literature. While a detailed description of such configurations is out of the scope of this paper, it is worth noting that, in all three cases, intense research has been done in optimizing DOFS configurations which can be used for sensing along fiber links compatible with standard installations of optical communication networks. This is an important advantageous

feature, as in this case, the DOFS systems can be used in fibers which are already installed without requiring additional infrastructures. Such configurations typically feature sensing ranges of tens of kilometres to more than 100 kilometres and spatial resolutions of a few meters using standard single mode fiber (SMF) [3–24].

However, the works presented in the literature rarely address the (in)compatibility between operating optical communication channels and DOFS. Due to the high powers used in typical DOFS, these systems cannot be trivially used in parallel with transmitted optical communication data, due to distortions induced in the signals. In general, these DOFS should require at least a dedicated optical channel for operation, but in fact, the requirement of a dedicated fiber for the distributed sensing is usually directly assumed. This will represent an additional (and often non-negligible) cost to the operation, as a dedicated fiber (or interruption of communications of an optical fiber) will be required. In the case of Rayleigh-based DOFS, the possibility of using the Rayleigh backscattering of transmitted data as a correlation OTDR (with an operation which was close to that of random CW lidars) has been proposed [25]. In this case however, the technique only allowed characterization of the losses/reflectivity of the fiber, similarly to noncoherent OTDR's [8,9].

In this paper, a technique is proposed to perform real-time distributed sensing of dynamic strain/vibrations using the reflection of live data of an operating optical communication channel. The technique is conceptually similar to a coded ΦOTDR employing an I/Q detection scheme. By taking advantage of the linearity of the sum of the Rayleigh backscattered complex electric fields, reflected by each optical bit in different places of the fiber, the impulse response of the fiber backscattering signal can be decoded. This allows for precise measurements of variations in the optical path along the fiber, thus allowing for distributed strain (and, in principle, also temperature) sensing with sampling rates limited by the size of the fiber, typically of several kHz. Note that the technique does not affect the operating communication channel, as it only requires a coherent detection unit to measure the channel's backscattered light (in amplitude and phase), provided that the transmitted data is known or measured. The proposed technique could be used to monitor intrusions or threats to the integrity of the physical fiber link. Since the sensing is performed at the same wavelength of the modulated data, this could be used in networks employing wavelength division multiplexing (WDM) [10,25].

2. Theoretical background and the proposed sensor

2.1 Traditional single-pulse ΦOTDR operation

DOFS based on optical time domain reflectometry (OTDR) work by inputting a pulse into an optical fiber and monitoring the backscattered light pattern in the time domain [1]. The signal $E(t)$ received at the fiber input ($z = 0$) at a time t, can then be associated to the light reflected around the fiber position z, by monitoring the light time of flight in the fiber [11]:

$$t = \frac{2n_g \cdot z}{c} \qquad (1)$$

where n_g is the fiber group refractive index and c is the velocity of light in the vacuum. In traditional OTDR-based sensing schemes the frequency f with which optical pulses are sent to the fiber is limited by the fiber round-trip time (RTT) ($f \leq 1/\text{RTT}$), thus avoiding the superposition of traces generated from different pulses. Here $RTT = 2n_g \cdot (\text{Fibre Length})/c$.

The operation of ΦOTDR is based on Rayleigh scattering and can be explained as follows: when a highly coherent optical pulse $P(t)$ [amplitude P_0 and central frequency ω] travels along the fiber, light is continuously (Rayleigh) backscattered by randomly (and densely) distributed fiber scattering centres. The signal $E(t)$ received at the fiber input ($z = 0$) will then be given by a superposition of the M waves, $E_m(t)$, Rayleigh backscattered from the M scattering centres existing in the fiber section $z = [t \cdot c/(2n_g) - W/2 , t \cdot c/(2n_g)]$, where W is the pulse width [11–13]:

$$E(t) = \sum_{m=1}^{M} E_m(t) = P_0 e^{i\omega t} \cdot \sum_{m=1}^{M} r_m e^{i\phi_m} \qquad (2)$$

where r_m is the reflectivity of the mth scattering centre, and ϕ_m the relative the phase of $E_m(t)$. Losses, dispersion or nonlinearities are neglected here for simplicity.

In a noncoherent OTDR, the relative phases of the reflected waves (Eq. (2) will vary randomly within a pulse and from pulse to pulse, and therefore will average to zero. In this case the measurement is only sensitive to optical intensity variations, which can be used to characterize the losses or locate fiber breaks [8,9]. In a ΦOTDR, however, due to the use of high-coherence pulses, the relative phases of the reflected waves will show a random but constant phase distribution along a pulse, and will remain constant from pulse to pulse, thus the signal $E(t)$ will be sensitive to changes in the relative phases ϕ_m of the reflected waves. These changes will typically be associated to refractive index changes caused by physical stimuli such as temperature or strain [14,15].

The intensity of $E(t)$, $I(t) = |E(t)|^2$, is commonly used to monitor vibrations/intrusions. However it is clear that the dependency of $I(t)$ on locally applied strain on the fiber is not linear, hence $I(t)$ is more effective in characterizing the frequency of an applied vibration, rather than quantifying its amplitude.

As for the phase of $E(t)$, it should vary linearly with the total optical path changes induced up to the correspondent fiber location z. In this case, the variations of the phase of $E(t)$ can be used to measure the integrated strain/temperature applied along the fiber, from which the local strain/temperature can be derived. However, it should be noted that while the variations of the phase of $E(t)$ will depend linearly on the strain/temperature variations applied before z, it will also depend nonlinearly on the strain/temperature variations locally applied in $z = [t \cdot c / (2n_g) - W / 2, t \cdot c/(2n_g)]$, due to the non-uniform variations of ϕ_m for waves reflected from scattering centres placed in different locations of this fiber section [23]. In this case, a ΦOTDR using phase detection should benefit from a high spatial resolution measurement (as the one proposed in this work), which would in principle enhance the importance of the linearity of the integrated strain/temperature variations and decrease the importance of the nonlinearity of the local strain/temperature variations.

Regarding sensing using ΦOTDR, the most common applications using ΦOTDR focus on the detection of vibrations/intrusions (distributed acoustic sensing). Taking advantage of the requirement for low averaging, high bandwidths of detection (limited by the fiber RTT) can be achieved: dynamic sensing with bandwidths ranging from 10's of kHz for a few kilometers [11,12], to 100's of Hz for more than 100 km (using distributed optical amplification) [16–20] have been demonstrated. With the use of detection schemes with phase recovery, the dynamic measurement of strain has also been demonstrated [21–23]. Note that several theoretical models describing the operation of ΦOTDR for different configurations and showing good agreement with the experimental results can be found in the literature [11–15].

Overall, the ΦOTDR operation using single frequency pulses has several characteristics which make for a suitable choice for implementation in parallel to operating optical communication networks. It uses a light source typically within range of linewidths (≈1MHz - 1kHz) employed in optical communications and is based on a linear effect (thus lowering the distortions induced to/by other signals propagating). However, traditional single pulse operation (with typical widths of ≈10ns-100ns) is not compatible with optical communication networks, where a continuous stream of high speed optical bits is transmitted. For this reason, we address below the possibility of using optical sensing with pulse coding techniques.

2.2 Coding in ΦOTDR

A common feature of DOFS in general, and OTDR schemes in particular, is that measurements have to be performed using backreflected signals of low power. Since the maximum peak power of the signal inputted to the fiber is limited by the onset of

nonlinearities, the power budget is typically one of the main limiting factors to set the maximum signal-to-noise ratio (SNR) and sensing distance of DOFS. Averaging of consecutive traces can be used to increase the SNR of the measurements, but this also increases the measurement time, impeding dynamic measurements. A more time-efficient way of increasing the SNR is with the use of pulse coding concepts [2–6,8,9,24].

As mentioned before, in traditional single-pulse OTDR based sensing schemes the frequency f with which optical pulses are sent to the fiber is limited by $f \leq 1/RTT$, in order to avoid the superposition of traces generated from different pulses. However, using pulse coding techniques, multiple pulses can be sent to the fiber within one RTT [2–6,8,9,24], thus increasing the total power inputted to the fiber, without increasing the pulse peak powers. In this case, the decoded trace will present a higher SNR for the same measurement time. Such techniques are particularly useful to increase the SNR of the trace at the end of the fiber (which can be used to increase the sensing distance), where the backscattered power reaches the minimum levels of detection. With the use of return-to-zero (RZ) simplex codes of length L, an SNR improvement of $(L + 1)/(2\sqrt{L})$ can be achieved [3,6,8,9], in comparison with traditional single pulse operation, for the same bit size.

A critical condition for employing pulse coding in DOFS is the linearity of the system [5,8]. It must be ensured that the addition of the traces generated from each bit is linear. Such condition is met when adding the optical intensities of traces in Raman OTDR [2,3], Brillouin optical time-domain analysis (BOTDA) [4–6] and noncoherent OTDR [8,9], where pulse coding techniques have been demonstrated using direct detection. In the case of ΦOTDR however, the addition of the optical intensities of optical traces is not linear, due to the coherent interference between traces backscattered from neighbouring bits [24]. In this case, when using intensity detection, distortions will be introduced in the decoding process and SNR improvement with the use of pulse coding is either not possible or strongly conditioned.

Under specific measurement conditions, the use of pulse coding has been recently demonstrated in a ΦOTDR using intensity detection [24] and RZ on-off keying (OOK): by precisely engineering the relation between the laser linewidth and the size/separation of the bits, so that the laser coherence length was higher than the bit size but lower than the bit separation, an improvement of SNR of up to ≈9 dB (255 bit) was achieved for the detection of low-power signals (without optical amplification in detection). However, the technique proposed in [24] was observed to allow decreasing the linewidth requirements of the master laser while maintaining the SNR of the measurement, but not increasing the SNR of a configuration using a high-coherence laser. An equivalent level of SNR was obtained when using an external cavity laser (ECL) with 50 kHz full width at half maximum (FWHM) with single pulse operation, as when using a distributed feedback laser (DFB) with 4 MHz FWHM and 255-bit cyclic coding. However, it was not possible to employ pulse coding when using the ECL of 50 kHz FWHM due to inter-pulse coherence. In any case, even if a low coherence laser is used, the technique proposed in [24] would not be suitable for implementation when using standard optical communication modulation formats, where the separation between optical bits is very small in relation to their size [or even zero, in non-return-to-zero (NRZ) modulation].

2.3 Proposed sensing method using coded sequences and I/Q detection

The proposed sensing scheme uses a continuous stream of optical bits as input signal $P(t)$ to the fiber, and a dual polarization I/Q detection unit which allows for a full (amplitude, phase and polarization) characterization of the backscattered optical signal $E(t)$. Compared to previously reported ΦOTDR configurations, as far as the authors know, this is the first time that the possibility of using arbitrary pulse coding in ΦOTDR as a fully linear system is proposed. The linearity of the system is derived from the fact that the sum of the optical fields reflected from each optical bit is linear (Eq. (2) – a condition which is not met for optical intensities - thus allowing for a linear decoding of the fiber backscattering impulse response. This allows for the use of modulation formats without restrictions in terms of bit separation (down to zero, i.e., NRZ), modulating frequency or modulating format (OOK, or different

types of phase-shift keying (PSK)/quadrature amplitude modulation (QAM)). Additionally, the input bit pattern does not have to be periodic. In this case, all the conditions required for performing ΦOTDR real-time sensing by simply monitoring the light backscattered from live data of an operating optical communications channel, are satisfied, as long as the transmitted pattern is known. The sensing can also be done without affecting the data transmission.

Regarding the spatial resolution, it is determined by (1/2) the bit size in the fiber, e.g., ≈2.5 cm for a 4 Gbaud modulation. Note that, in principle, there is no limitation in terms of minimum bit size (i.e., maximum modulating frequency) or bit separation required in ΦOTDR, unlike BOTDA schemes, in which a minimum bit size (≈10 ns) and bit separation (≈60 ns) is required, owing to the properties of acoustic waves in the fiber [5]. Therefore, in principle, a much higher number of bits (and therefore SNR gain) can be achieved in comparison with those typically demonstrated so far for DOFS (typically of up to 511 bits, i.e., a SNR increase of up to ≈10.5 dB [3,6,9]). However, care has to be taken when going to high frequency modulations as it is necessary to control the noise in the pulses. Note that the tolerance for bit distortions is lower from the sensing point of view (as these will introduce distortions in the trace decoding process) than from the communications point of view, where the bit-error rate can be low even after significant distortions.

While different modulation formats can be used in the proposed technique, experimental results were focused in PSK, as this modulation is advantageous for both communications and sensing. For communications, the use of PSK/QAM formats allows for a higher spectral efficiency than OOK, and is currently becoming a standard for high capacity optical networks. As for sensing, compared to OOK (where on average 1/2 of the bits are "0") the use of PSK allows to effectively double the optical power launched into the fiber, while maintaining the same peak power. This allows for a theoretical increase of the SNR by a factor of √2 [4], without a significant impact in nonlinearities, which are mostly related to the signal peak power. The use of NRZ PSK modulations therefore allows to achieve the ultimate power input to the fiber: a continuous flat temporal power limited by the nonlinearities. Additionally, due to the existence of sequences of "0"s of different lengths, OOK can lead to inhomogenities in the peak powers of the optical bits after the amplification stages, which introduce errors in the decoding of the trace. Such problem is avoided with PSK, since a constant power input to the amplification stages will ensure that the amplitude of all the bits is constant (or will present much lower fluctuations).

The coding/decoding of the fiber trace using non-periodical PSK modulation formats can be explained similarly to periodical OOK modulation. For simplicity, for a given bit size τ_{bit}, we assume that the detection sampling rate is $1/\tau_{bit}$ (i.e., the detection provides one sample point per bit), and the fiber $RTT = (N + 1) \cdot \tau_{bit}$. The fiber impulse response for a "standard" single bit (of amplitude $A = 1$ and phase shift $\phi = 0$), i.e., the Rayleigh backscattered signal when a "standard" single bit is launched to the fiber is defined as $r(t)$. The detected $r(t)$ is therefore a discrete array with N points, $r(t_n)|_{[n=0,N]}$. For $n<0$, $n>N$, then there is no reflection, i.e., $r(t_n) = 0$ (as the bit is not yet in, or already out of the fiber). If a generic bit of amplitude A_0 and phase shift ϕ_0 is inputted to the fiber, then the Rayleigh backscattered signal $E(t_n)$ will still be an array of $N + 1$ points, which will now be given by:

$$E(t_n) = A_0 e^{i\phi_0} \cdot r(t_n) \quad ; \quad n=[0,N] \tag{3}$$

It can then be directly derived that if two consecutive bits 0,1, where bit 0 is delayed by τ_{bit} from bit 1, are launched into the fiber, then $E(t_n)$ will now be given by:

$$E(t_n) = (A_0 e^{i\phi_0}) \cdot r(t_n) + (A_1 e^{i\phi_1}) \cdot r(t_{n+1}) \quad ; \quad n=[0,N] \tag{4}$$

The generic $E(t_n)$ received during a fiber RTT for a continuous stream of bits, is then described by the matrix eq.:

$$\begin{pmatrix} \mathrm{E}(t_0) \\ ... \\ \\ \mathrm{E}(t_N) \end{pmatrix} = \begin{pmatrix} A_0 e^{i\phi_0} & A_1 e^{i\phi_1} & ... & A_N e^{i\phi_N} \\ A_{-1} e^{i\phi_{-1}} & A_0 e^{i\phi_0} & ... & ... \\ ... & ... & ... & A_1 e^{i\phi_1} \\ A_{-N} e^{i\phi_{-N}} & ... & A_{-1} e^{i\phi_{-1}} & A_0 e^{i\phi_0} \end{pmatrix} \cdot \begin{pmatrix} r(t_0) \\ ... \\ \\ r(t_N) \end{pmatrix} \Leftrightarrow E(t) = (\mathrm{P} * \mathrm{r})(t) \quad (5)$$

In Eq. (5), $P(t)$ should be known (input bit stream) and E(t) should be measured, so that $r(t)$ can be calculated. It should be noted that even with a non-periodical signal, a measurement of the state of the fiber [i.e., calculation of the fiber impulse response $r(t)$] at the rate of 1/RTT can in principle be performed, as long as a bit stream of length $\approx 2 \cdot \mathrm{RTT}$ (2N + 1) is known.

With the number of bits N easily reaching tens of thousands, it is clear that solving Eq. (5) using straightforward matrix operations requires a large computational power and memory. However, even with the use of live (random non-periodical) data, smarter decoding procedures can be engineered, as the information contained in Eq. (5) is essentially composed of 1D arrays of the size of $r(t)$ [26].

If the use of live data is not required and the bit sequence can be freely chosen, then much simpler and faster decoding processes can be engineered. For e.g., for a cyclic PRBS pattern, the decoding $r(t)$ can be performed by simply using:

$$r(t) = \mathrm{iFFT}\left(\frac{\mathrm{FFT}\left[E(t)\right]}{\mathrm{FFT}\left[P(t)\right]}\right) \qquad (6)$$

The use of a cyclic PRBS pattern provides an optimal solution in this case as it will present an optimal flat spectral power distribution. This requirement stems from the need of minimizing zeros in the denominator of Eq. (6), which would lead to high numerical errors in the recovery of $r(t)$.

An extensive mathematical study on the dependency of the decoding errors on the properties of the matrix $P(t)$, which will affect the determination of $r(t)$, and therefore the SNR of the fiber measurement, is out of the scope of this paper. However, for a large set (tens of thousands) of random bits, a well behaved spectral distribution is expected and the errors induced in the demodulation process should not be critical. As we will see later, the results obtained using a cyclic PRBS pattern by solving Eq. (6) (section 4/5) are comparable to those obtained with random live data (section 6) using a least squares channel estimation method [26].

3. Experimental setup

The schematic of the experimental setup used is shown in Fig. 1. It is based on real-time measurements of the complex backscattered field (phase, amplitude and polarization) of data signals modulated using PSK that are launched into the fiber. In terms of the light source requirements, the setup is completely comparable to a regular transmitter setup used in coherent communication systems.

An external cavity laser (ECL) [RIO Planex] with a linewidth of ≈ 1 kHz and emitting at 1550.12 nm was used as a high coherence continuous wave (CW) light source. The CW was split by a 90/10 coupler where the 10% of the CW was used as a local oscillator (LO) for the I/Q detection, after being amplified and passing through a polarization controller (PC), and the 90% of the CW passed through a PC and was then modulated by a Mach-Zehnder modulator (MZM) [from SHF AG] which had a bandwidth of 40 GHz and was controlled by a signal generator (SG). The modulation format was binary PSK (BPSK) and the symbol rate was of 4 Gbaud. An erbium-doped fiber amplifier (EDFA) was used to amplify the data to an average power of 18 dBm before being launched into the fiber through a circulator. The EDFA had a signal output which was monitored with a photodetector + oscilloscope and allowed to adjust the working point of the MZM.

The fiber under test (FUT) consisted of a roll of 500 m of standard single-mode fiber (SMF). Near the end of the FUT a fiber section was attached to a PZT which allowed to apply controlled deformations to the fiber.

The backscattered signal was amplified with another EDFA. After this, a filter with a spectral width of ≈0.3 nm (≈40 GHz) was used to remove the amplified spontaneous emission (ASE). A PC and an attenuator were used to optimize the polarization and power of the backscattered signal before detection.

The detection system consisted of a dual-polarization coherent receiver [u2T CPRV1220A] - an integrated module with four balanced detetors and transimpedance amplifiers (TIAs) and 90 degree hybrid. A digitizer (bandwidth 62 GHz) [Agilent, DSO-X 96204Q], synchronized with the MZM SG driver, recorded the I/Q signal backscattered from the fiber in both (x,y) polarizations, with a sampling frequency of 20 GHz. These signals were then down sampled to 8 GHz by software. Considering the 4 Gbaud modulation, it should be noted that the high bandwidth of the detection scheme is not a requirement for this setup (and will in fact add additional noise to the measurement without benefits in detection).
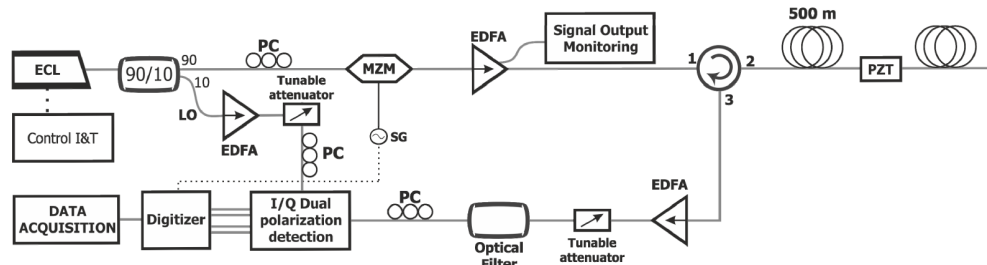

Fig. 1. Experimental setup: Acronyms are explained in the text.

4. ΦOTDR trace and signal polarization rotation

The feasibility of using transmitted data modulated at high frequencies to perform distributed sensing was experimentally studied. For a 500 m fiber, the fiber RTT is of ≈4.9 μs, which corresponds to 19560 BPSK bits modulated at 4 Gbaud and 39120 points sampled at 8 GHz. In order to perform a set of experimental results which provide a conceptual demonstration of the use of high-speed modulated data to perform distributed sensing without being limited by computational power, a cyclic pseudorandom binary sequence (PRBS) was used for the modulation of the bits. The pattern length of the PRBS was 2^{15}-1 bits and the fiber was therefore sampled with a period of 8.19175 μs (correspondent to a RTT of a fiber of about 840m). The fiber impulse response $r(t)$ was then decoded using Eq. (6).

Figure 2(a) and 2(b) show the optical power distribution of the ΦOTDR trace (i.e., decoded backscattered fiber signal) received in the x and y polarizations, respectively. A moving average of 10 traces in the temporal domain was used. As expected, the trace presents a similar signal to a traditional single pulse ΦOTDR trace, but with a higher SNR. A detailed characterization of the SNR gain due to the use of coding is out of the scope of this paper. However, the SNR gain is notorious, as a traditional single pulse ΦOTDR using a 0.25ns pulse (to achieve the 2.5 cm spatial resolution presented here) would present serious operational problems due to the noise. Note that for a code of length N = 2^{15}-1, if no impairments are imposed by other factors related to the use of coding, the theoretical gain G in SNR (using PSK) due to the use of coding would be:

$$G = \frac{N+1}{\sqrt{2}\sqrt{N}} \approx 21\,\mathrm{dB} \tag{7}$$

In Fig. 2, the rotation of the polarization state of the ΦOTDR signal along the fiber is described in a clear and highly visual manner. In this case, apart from the typical jagged appearance of the ΦOTDR trace, Figs. 2(a) and 2(b) show a slowly varying envelope

function, which maximizes/minimizes the optical intensity detected at one polarization axis, when the ΦOTDR signal polarization is aligned/misaligned with that axis. Figure 2(c) shows a zoom of the superposition of the x and y-polarization ΦOTDR signal, putting in evidence that the maxima of one polarization are coincident with the minima of the other, i.e., when the signal is misaligned with one polarization, it is aligned with the other. Figure 2(d) shows the sum of the optical intensities received in both polarizations, showing that the overall optical power is kept constant when using diversity polarization detection. The average period of polarization rotation (i.e., distance between consecutive peaks of Figs. 2(a) and 2(b)), was observed to be ≈15 m which is in agreement with the expected values of beat length for an SMF.
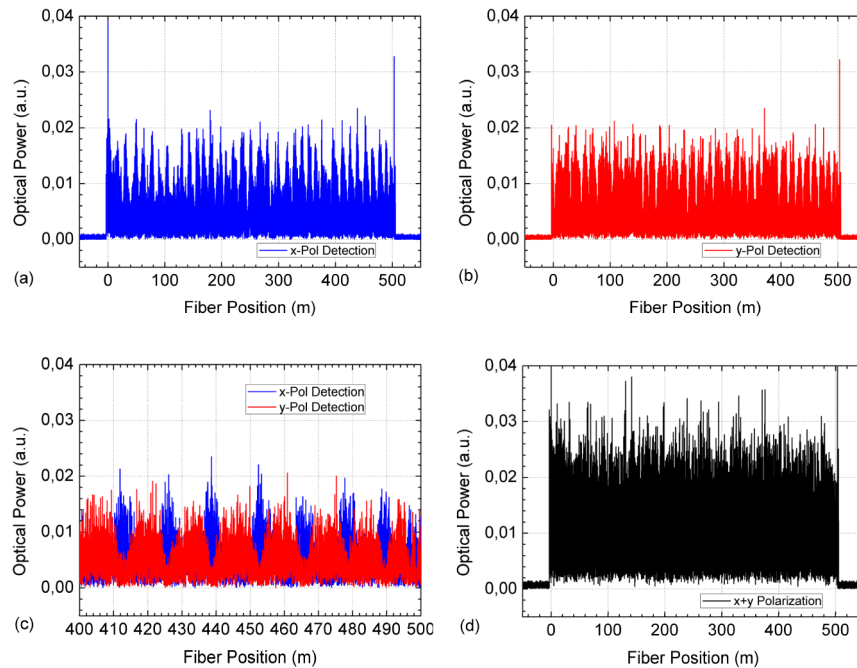

Fig. 2. Optical Power of ΦOTDR decoded signal along the fiber launching single polarization BPSK data. (a) Signal detected on the x polarization. (b) Signal detected on the y polarization. (c)Zoom of superposition of x and y polarization signals (d)Sum of x and y polarization signals

5. Dynamic distributed strain measurements

The measurement of distributed dynamic strain with the proposed system was characterized. Firstly, in order to characterize sensing over continuous fiber sections, strain was applied over a fiber section of 5m. Then, in order to characterize the spatial resolution and linearity of the sensor, precisely controllable strain variations were applied over fiber sections of the order of the spatial resolution (a few centimetres).

For the first part, a fiber section of 5m, near the end of the 500m fiber, was wrapped around a homemade PZT, in a total of 15 fiber loops. The fiber loops had a length of ≈33cm (i.e., ≈13 resolvable points) and were glued to the PZT in the beginning and end, so that strain could be applied independently to each loop. The fiber loops were alternated between loose loops (where strain was not applied), and tight loops (where strain was applied). The tight loops had a pre-tension and therefore equal strain variations were applied to each tight loop. The sequence of loose (marked as 0) and tight (marked as 1) loops was: 110010101010011. The phase of the ΦOTDR signal was then monitored when the PZT strain was changed. Since the ΦOTDR signal presented a high SNR and the polarization extinction ratio was not very high (i.e., the minima of Figs. 2(a)/2(b) still presented measureable signal) the strain

measurements were performed using only one polarization ΦOTDR signal, for simplicity. However, it should be noted that the processing of ΦOTDR signal taking into account both polarization channels should allow for the SNR to be higher and more even along the fiber. Figure 3 shows a plot of the phase variation of the ΦOTDR signal between two measurements of the fiber around the location of the PZT. The two measurements, separated by 1 ms, correspond to a case where the PZT was strained and unstrained. The variation of the phase of the ΦOTDR signal along the fiber was as expected: the phase remained constant in the loose fiber sections where strain was not applied and increased linearly in the tight fiber sections where strain was applied. The phase variations at a given point of the fiber were therefore linearly related to the total integrated deformation variation applied before that point.
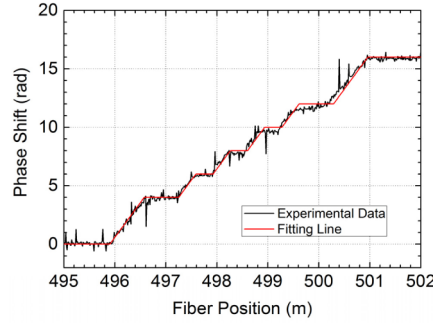

Fig. 3. Phase variation recovered around the location of the PZT, comparing two fiber measurements where the PZT was strained and unstrained.

For the second part, strain was applied to 3 fiber sections of lengths 2.5cm/5cm/2.5cm, labeled as section 1,2,3, respectively. These were separated by ≈20 cm and were located near the end of the 500 m fiber. The beginning/end of each of the three fiber sections was glued to the same fixed/moving part of a commercially available horizontal translation stage. The position of the stage was controlled by an electric signal, which allowed to apply precisely controllable strain variations. In this case, the deformations applied to each fiber section were the same, but the strain in section 2 (5 cm) was half of that applied in sections 1,3 (2.5 cm).

Figure 4(a) shows the phase variation of the recovered ΦOTDR signal along the fiber between two measurements, when strain is applied to the three fiber sections. As expected, the total phase shift after each section is approximately the same (2 rad). A small discrepancy in the phase shift (≈0.2 rad) is observed in the fiber section 2, which could be owned to insufficient pre-strain applied to the fiber, or small fiber drifts occurring in the points where the fiber was glued.

Figure 4(b) shows the strain calculated from the spatial derivative of the phase plots of Fig. 4(a). Since the optical resolution was of 2.5cm (4 GHz bits) and the sampling resolution was of 1.25 cm (8 GHz), the strain was calculated as follows: firstly, a moving spatial average of 2 points of the ΦOTDR signal phase was calculated, then the phase difference $\Delta\phi(z)$ between the signal of fiber points separated by $\Delta z = 2.5$ cm was calculated. The strain along the fiber $\varepsilon(z)$ was then obtained using:

$$\varepsilon(z) = \frac{\lambda \cdot \Delta\phi(z)}{n \cdot (2\Delta z) \cdot 2\pi} \tag{8}$$

where $\lambda = 1550$nm is the signal wavelength and $n \approx 1.467$ the effective refractive index of the fiber.

A good agreement between the measured and applied strain both in spatial distribution and amplitude was observed in all three sections. For the first section, a small discrepancy is observed as the measured strain is distributed along a slightly larger section (one more sampling point) and therefore presents a lower amplitude. Note that due to the random nature

of the ΦOTDR, the signal can present errors at certain specific fading points, where the signal intensity is very low. However, given the relatively low probability of occurrence of these points, the error introduced by these points can be eliminated or greatly reduced by the use of smoothing functions. In any case, the strain measured was qualitatively and quantitatively as expected and the theoretical spatial resolution of ½ the size of one optical bit (≈2.5 cm) was clearly demonstrated. This is more than one order of magnitude below the typical maximum spatial resolution achievable for traditional single pulse ΦOTDR, which struggles to achieve submeter spatial resolutions [12].
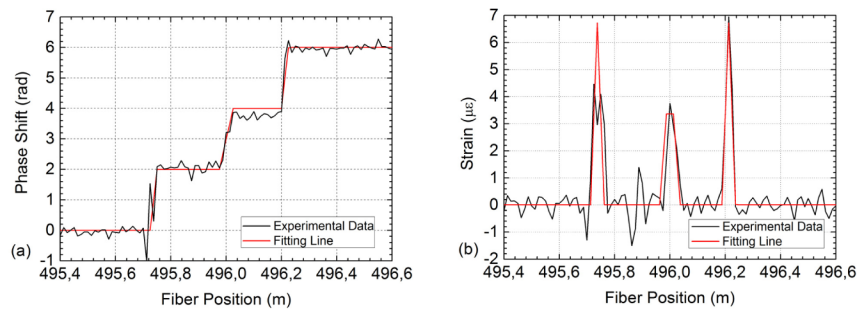

Fig. 4. (a) Phase variation of the ΦOTDR signal along the fiber when strain is applied in three fiber sections 1,2,3 of length 2.5cm/5cm/2.5cm by a translation stage. (b) Correspondent calculated strain variation along the fiber.

Figure 5(a) shows the phase variation of several points, before, at and after the strained fiber sections when a sinusoidal strain variation of 500 Hz was applied by the translation stage. The plots labelled as "at the fiber section X" are correspondent to the sampling point placed in the middle of the section X, while the plots labelled as "before/after section X", are correspondent to a point placed before/after the strained sections (the phase plots of the points placed outside the strained sections were observed to be equivalent, as observed in Fig. 5(b)). It was observed that the linearity of the strain-phase variations is better when monitoring points after, rather than at, the location where the strain is applied. This is in agreement with previous reports [23] and the theoretical expectations (discussion following Eq. (2), but it could also be related to the fact the strain is applied over a fiber section very close to the spatial resolution. Note that for the section 2 (5 cm) the linearity is significantly better than in the sections 1,3 (2.5 cm). In any case, a good overall linearity is observed in all points.

Note that variations of deformations/strain correspondent to phase variations arbitrarily larger than 2π can be measured, as long as the sampling of the fiber is fast enough and the spatial resolution small enough to avoid jumps of more than $\pm\ \pi$ between consecutive (spatial or temporal) points, thus allowing for a correct unwrapping of the ΦOTDR phase function. This can be clearly understood by observing the 3D representation of the phase variation of the fiber along time (Fig. 5(b)).
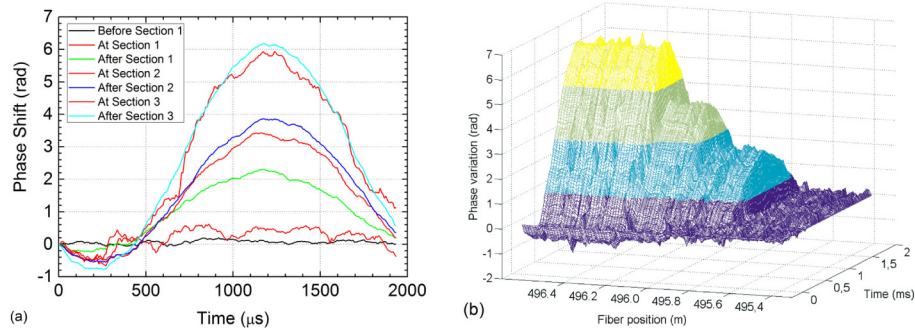
Fig. 5. Phase variation of the ΦOTDR signal when a 500 Hz strain variation is applied to the fiber sections 1,2,3. (a) Phase variation of different points over time (b) 3D representation of the phase variation along the fiber over time.

6. ΦOTDR using QPSK dual polarization and random data

After demonstrating the possibility of the use of our technique for distributed strain sensing using the reflection of BPSK data with a single polarization, the flexibility of the proposed technique is conceptually illustrated by using dual polarization QPSK.

In order to generate the dual polarization QPSK data, an additional step was added to the setup described in Fig. 1 before the data was launched into the fiber. The CW linearly polarized light was modulated into a QPSK signal (using a modulation scheme with two MZM). Then, the light was split by a 50/50 coupler and the polarization of the signal on one of the arms was rotated by 90° and delayed by ≈1.16 µs (light was passed by a fiber of length ≈238 m). A polarization beam combiner was then used to recombine the signals of polarizations x and y, before launching it into the fiber. The detection scheme was the same as described in Fig. 1. Provided that the polarization optical delay is larger than the channel impulse response (i.e., the RTT of the FUT to be measured), this effectively provides a dual polarization signal with two independent codes being used on each polarization. The 500m FUT was replaced by a 70 m FUT (RTT ≈0.88 µs).

Figure 6 shows the optical power distribution of the ΦOTDR trace for the 4 cases (2x2) correspondent to 2 polarizations of launching signal and 2 polarizations of detection. Figure 6(a) (respectively 6(b)), corresponds to the ΦOTDR trace detected on the x (respectively, y) polarization, when data is launched into the fiber on the x polarization. Figure 6(c) (respectively 6(d)), corresponds to the ΦOTDR trace detected on the x (respectively, y) polarization, when data is launched into the fiber on the y polarization. Note that the ΦOTDR trace signals $r(t)$ of Fig. 6 were obtained by directly solving Eq. (5), using the signal the signal received on the x,y polarizations as E(t), and the data codes applied to the x,y polarizations as P(t).
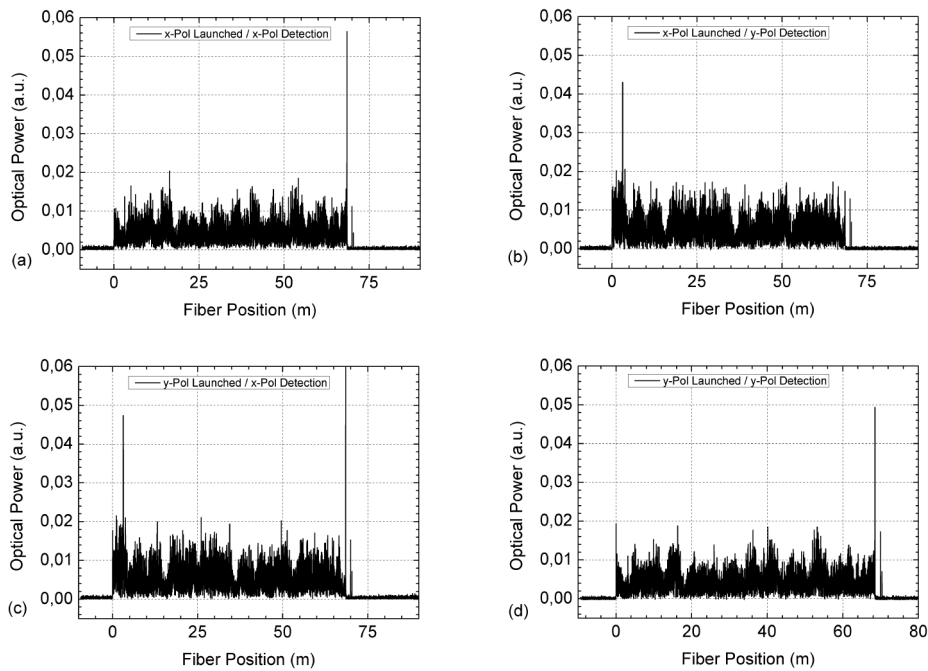
Fig. 6. Optical Power of the ΦOTDR decoded signal along the fiber launching dual polarization QPSK data. Figures show the impulse response of the fiber when data is sent on the **x** polarization and detected on the (a) x polarization (b) y polarization; data is sent on the **y** polarization and detected on the (c) x polarization (d) y polarization.

The results shown in Fig. 6 can be explained as follows. If data is launched only on one polarization, a situation equivalent to the described in section 4 should be obtained. Therefore, Fig. 6(a)/6(b) and Fig. 6(c)/6(d), show a similar result to the observed in Fig. 2(a)/2(b), with complementary maxima/minima of the trace being detected on the x/y polarizations (due to polarization rotations). Additionally, since pulses launched into the fiber on orthogonal polarizations will remain orthogonal as they propagate along the fiber (assuming that for the short distances used coupling between polarizations is negligible), the traces detected on one polarization for data launched on orthogonal polarizations should also show complementary maxima/minima. For this reason, maxima/minima of Fig. 6(a) are complementary to 6(b) and Fig. 6(c) are complementary to 6(d). Since the used fiber (SMF) had low birefringence, then a similar signal should be detected on the X polarization (respectively Y) when data is sent on the X polarization, as detected on the Y polarization (respectively X) when data is sent on the Y polarization. For this reason, Fig. 6(a) is similar 6(d) and 6(b) is similar to 6(c). Overall, the traces obtained were as expected in all cases, demonstrating the possibility of performing measurements with QPSK data which, in theory, could include birefringence characterization.

In order to provide a comparison ground with the results obtained using single polarization BPSK, a sinusoidal strain variation of 500 Hz was applied by the translation stage using the same settings as those used in Fig. 5(a). Apart from the modulation format, the only difference was the fiber size used before the PZT (500 m in Fig. 5(a), and 70 m in Fig. 7). The measured phase variation of different points over time is shown in Fig. 7. The presented results clearly demonstrate that the proposed approach is valid for arbitrary data modulation formats, using random data comparable to that obtained in real communication links.
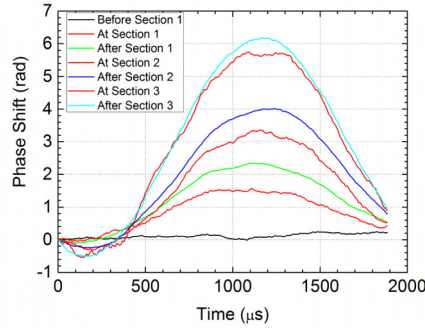
Fig. 7. Phase variation of the ΦOTDR signal over time for different fiber points when a 500 Hz strain variation is applied to the fiber sections 1,2,3, using the same settings as Fig. 5(a), but using a dual polarization QPSK data format.

7. Considerations on the proposed technique trade-offs and limitations

The variation of the ΦOTDR signal phase measured at a certain point of the fiber will be determined by the integration of the optical path variations occurring along the entire fiber (due to strain or temperature variations) and/or phase drifts/noise between the LO and signal backscattered from the fiber. Considerations regarding the impacts of the different phase noises and maximum tolerable ΦOTDR signal phase variations are presented below.

7.1 Laser source requirements

Regarding the laser source, an important feature is that its coherence length should be higher than twice the fiber length, in order to avoid phase noise being introduced in the measurement when beating the LO and signal backscattered from the fiber. While this will increase the laser requirements for long fibers, commercially available lasers can reach linewidths below 1 kHz (coherence length of ≈100km) and therefore this should not be a major limitation for fibers of up to 50 km.

As for the frequency drifts occurred between the LO and the backscattered signal (caused by frequency drifts of the laser source over time), these will cause a small continuous phase drift of the ΦOTDR measured signal. Again, commercially available lasers can be quite stable in frequency, and therefore this effect can be made small, even for fibers of tens of km. In this case, this effect would most likely be masked as a small average temperature variation along the fiber, which should not affect the local measurement of strain.

7.2 Fiber optical path variations occurring **between** fiber measurements (**over a time >RTT**)

Regarding the accumulated temperature/strain changes along the fiber, these can easily lead to optical path changes exceeding 2π between consecutive measurements even for relatively short fibers. For a standard SMF the refractive index change Δn occurred for temperature variation ΔT is given by $\Delta n \approx 10^{-5}\Delta T$ [14]. Therefore, the phase variations $\Delta\phi$ of the ΦOTDR signal backscattered from the end of a fiber of size L, using a laser source of wavelength λ, due to an average fiber temperature change ΔT will be given by [14]:

$$\Delta\phi = 2\pi\frac{2L \cdot \Delta n}{\lambda} \approx 2\pi\frac{2L \cdot (10^{-5}\Delta T)}{\lambda} \qquad (9)$$

This means that, in the presented setup (L = 500m, λ = 1.55 μm), a $\Delta\phi \approx 2\pi$ would be obtained for $\Delta T \approx 1.55*10^{-4}$K. It is therefore clear that the variation of the absolute phase of the ΦOTDR signal reflected from the end of the fiber can (and is in fact expected to) vary by values much larger than 2π, over measurements of only a few seconds due to a small

fluctuations of the average fiber temperature. However, in order for the temporal/spatial variations of the phase of the ΦOTDR signal to be correctly unwrapped, it is only necessary to ensure that variations larger than $\pm\,\pi$ do not occur between consecutive spatial points of consecutive measurements. In any case, a number of post-processing methods to eliminate these low frequency variations of the ΦOTDR signal phase along the fiber can be thought of. For example, the derivative of the phase profile (i.e., the instantaneous frequency, directly related to the applied strains) or the difference between the phase variations of relatively close fiber points could be used.

An important note is that the requirement of keeping the local phase variations smooth will set a limitation for the maximum measurable local strain variations which will scale with the fiber temporal sampling (i.e., the RTT of the fiber) and the spatial resolution (i.e., the bit size). With the presented setup, it can be derived from Eq. (8) that a maximum strain of $\approx\pm\,10\mu\varepsilon$ (correspondent to $\Delta\phi = \pm\,\pi$, over 2.5cm) occurring between two consecutive measurements (i.e., $\approx 8\mu s$), could be measured. Still, if a large strain variation occurs at a given point, this should not affect greatly the overall quality of the strain measurements along the rest of the fiber.

7.3 Fiber optical path variations occurring **during** a fiber measurement (**over a time <RTT**)

The considerations presented in points 7.1 and 7.2 are generically also valid for traditional single pulse ΦOTDR systems using phase as the measurement parameter. However, the use of a continuously modulated data inputted to the fiber gives rise to an additional limitation which is not particularly relevant in traditional single pulse ΦOTDR: the fiber needs to be static during at least the fiber RTT, i.e., the time over which a fiber trace measurement is performed.

This can be observed in Eq. (5): the fiber state $r(t)$ is assumed to be constant over the duration over which $E(t)$ is received. If a phase drift $\Delta\phi > 2\pi$ occurs along the fiber while the data used to interrogate the fiber is still traveling along the fiber, then the backscattered signal $E(t)$ will be distorted and the decoding process will introduce important distortions in the recovered $r(t)$. The impact of this effect is greatly dependent not only on the fiber size, but also on the fiber perturbations occurring during the measurement time. While further work on the limitations of the system due to this effect should be done, preliminary tests show that, for example, applying air currents to a fiber roll of as little as 1km of length can lead to significant distortions.

Strictly from the sensing point of view, an intermediate solution to this effect can be used between the traditional single-pulse ΦOTDR and the proposed ΦOTDR using continuously modulated data: the use of a ΦOTDR which uses a finite train of coded pulses. This would lower the coding gain (as the coding sequence is smaller), but, in this case, the fiber is only required to be static over the duration of the pulse train, rather than the fiber RTT. This, however, cannot be implemented using the reflection of optical communication channels, as the transmission of data cannot be continuous.

8. Conclusions

A technique that allows using the reflection of live data of an operating channel to perform real-time distributed strain sensing has been proposed and experimentally validated. The technique is conceptually similar to a coded ΦOTDR employing an I/Q detection scheme and offers the possibility for strain (and, in principle, also temperature) sensing with cm resolutions over tens of km with sampling rates of several kHz. The required light source is completely comparable to a regular transmitter setup used in coherent communication systems using standard data modulation formats and the technique does not affect the operating communication channel. Efficient decoding procedures can be proposed to keep the required computational power bounded, since the information to be handled is essentially linearly proportional to the size of the fiber.

In this work, as a proof of concept, using 4 Gbaud random and non-periodical NRZ single-polarization BPSK and dual-polarization QPSK, distributed sensing of dynamic strain with a sampling of 125 kHz and spatial a resolution of 2.5 cm over 500 m is demonstrated for applied sinusoidal strain signals of 500 Hz. However, further work should be done in characterizing the system limitations under different configurations, mainly the maximum measurable fiber distance (and if/how it is limited by the occurrence of phase drifts during the measurement time, as discussed in 7.3), and distortions induced to/by other signals propagating (which should be minimal in the linear regime for low powers) should be evaluated.

Beyond the telecom domain, the proposed technique could be extensively used in distributed optical fiber sensing. Lower bit rates and lower detection bandwidths could be used to reduce both the cost of the system and the noise in detection. Also, in principle, there is no limitation as for the maximum bit modulation frequency (spatial resolution) or bit separation (down, to zero, i.e., NRZ data). Therefore, the SNR and maximum resolvable sensing points (high spatial resolutions over large ranges) could be greatly increased when compared to traditional single pulse ΦOTDR operation. For example, using 10 Gbaud (1 cm) over 10 km, a configuration breaking the 1 000 000 resolvable sensing points could be achieved.

Acknowledgments